

Magneto-optical Kerr spectroscopy of palladium

A. N. Yaresko,* L. Uba,[†] S. Uba, and A. Ya. Perlov*

Institute of Physics, The University in Bialystok, Lipowa 41, PL-15-424 Bialystok, Poland

R. Gontarz

Institute of Molecular Physics, Polish Academy of Sciences, Smoluchowskiego 17, PL-60-179 Poznan, Poland

V. N. Antonov

Institute of Metal Physics, 36 Vernadskii Street, 252142 Kiev, Ukraine

(Received 2 April 1998)

Magneto-optical Kerr effect (MOKE) spectra of a paramagnetic fcc Pd metal film, measured with high sensitivity in an applied magnetic field of 1.5 T over a photon energy range 0.8–4.8 eV, are presented. *Ab initio* linear-muffin-tin-orbital calculations reproduce the experimental spectra well, and explain the microscopic origin of the magneto-optical (MO) response in terms of the individual interband transitions. A band-by-band decomposition of the fcc Pd MO spectra is presented, and transitions responsible for prominent structures in the spectra are identified. The dominant role of transitions from states in the vicinity of the Fermi level is found. It is found and explained that the proportionality between the magnitude of the MOKE spectra and the magnetic moment induced on the Pd atom holds over two orders of magnitude up to the value of $\sim 0.25\mu_B$ typical for magnetic Pd compounds. It is shown that, in spite of the different mechanisms of the Pd magnetization, the MOKE spectra of the paramagnetic Pd metal in the external magnetic field are similar to the spectra of the ferromagnetic diluted Co-Pd and Fe-Pd alloys. [S0163-1829(98)01036-4]

I. INTRODUCTION

In the past decade, a large number of studies have been conducted for multilayer and alloy films consisting of magnetic transition metals and Pd or Pt using various experimental techniques.^{1–5} These systems exhibit simultaneously enhanced magneto-optical Kerr rotation in the uv spectral range¹ and perpendicular magnetic anisotropy²—a combination of properties which allows the use of these materials as a recording medium in a new generation of storage devices.³ Most measurements of these systems give indirect evidence of a large spin polarization of Pt and, especially, of Pd at Co,Fe/Pd,Pt interfaces in the layered structures,⁴ as well as in the vicinity of magnetic impurities in the diluted alloys.⁵ The underlying mechanism of the Pd(Pt) magnetism in these systems is usually interpreted in terms of strong $3d$ - $4d$ ($5d$) hybridization and the exchange interaction.

On the other hand, Pd itself is very interesting. Pd metal is nearly ferromagnetic, with the largest paramagnetic susceptibility among the nonmagnetic transition metals, and is easily spin polarized by a small external magnetic perturbation. Due to the high density of electronic states at the Fermi level, the bulk fcc Pd metal is near the threshold of becoming ferromagnetic, and calculations predict a paramagnetic-ferromagnetic phase transition upon the lattice expanding by 6%.⁶ The unique properties of Pd stimulated a large number of experimental and theoretical investigations (see, e.g., Ref. 7 and references therein).

Magneto-optical Kerr effect (MOKE) spectroscopy is a useful experimental technique for investigating the electronic structure of magnetic materials, and there is currently a great deal of activity to understand the origin of magnetic-optical (MO) effects in various systems. Of key importance to the

understanding of the attractive magneto-optical properties of Co and Fe-Pd systems is the investigation of the Pd MO response and its contribution to the MOKE spectra under various circumstances. The MOKE spectra are related to subtle electronic structure effects such as the hybridization, the magnitude of exchange polarization, and the spin-orbit coupling. The spin polarization of Pd was used tentatively to interpret qualitatively the observed MOKE enhancement in the Co,Fe-Pd compounds. An attempt at an investigation of the MO properties of Pd has been undertaken by Reim *et al.*,⁸ who considered the MOKE spectra of a Pd_{0.94}Fe_{0.6} alloy as mainly due to the MO response of spin-polarized palladium. They found that, neglecting the magneto-optical activity of iron atoms, Pd is characterized by off-diagonal conductivity tensor components of the same order of magnitude as for $3d$ ferromagnetic materials.

Such indirect investigations cannot give a complete picture of the MO properties of Pd. In our opinion, exhaustive information can be obtained only by direct measurement of the MOKE spectra of pure Pd metal, together with *ab initio* band-structure calculations, which have been successfully applied to describe the MO properties of a wide class of ferromagnetic materials in the last years.⁹

The paper is aimed at experimentally and theoretically investigating the MO properties of paramagnetic Pd in an external magnetic field. The MOKE spectra of the fcc Pd metal film, measured with high sensitivity in an applied field of 1.5 T over the spectral range 0.8–4.8 eV, are presented and compared to the spectra of Fe_{0.06}Pd_{0.94} and Co_{0.13}Pd_{0.87} alloys. The origin of the Pd MOKE spectra is analyzed in terms of the individual interband optical transitions, as derived from first-principles calculations. It is found that the amplitude of the MOKE spectra is proportional to the value

of the magnetic moment induced on the Pd atom. In contrast to the case of ferromagnetic diluted alloys, where the Kerr effect is due to the simultaneous occurrence of the spontaneous exchange splitting and the spin-orbit coupling, the Kerr effect induced by an external magnetic field in the paramagnetic Pd (which has zero spontaneous exchange splitting) is due to a rather different mechanism. The dependence of the MO properties of magnetized Pd on the source of the magnetization is discussed.

II. MAGNETO-OPTICAL PROPERTIES OF PARAMAGNETIC PALLADIUM

To investigate the magneto-optical response of Pd metal itself, we measured the polar MOKE spectra of paramagnetic Pd in an external magnetic field of 1.5 T over the photon energy range $0.8 < \hbar\omega < 4.8$ eV. Thick (~ 2000 Å) polycrystalline fcc Pd films were prepared using the dc sputtering deposition system described in Ref. 10. The polar Kerr effect induced in Pd by a magnetic field of 1.5 T is very small (below 10^{-3} deg), and was detected in a sensitive Kerr spectrometer setup¹¹ by means of a polarization modulation technique using a piezobirefringent modulator. Besides a high sensitivity reaching the 10^{-5} – 10^{-4} deg range (depending on the photon energy and corresponding photon shot noise), this method has the advantage that the Kerr rotation and Kerr ellipticity can be determined simultaneously. The acquisition time was long enough to obtain a sufficiently large signal-to-noise ratio. The measurements were repeated a number of times on different samples, and the resulting spectra presented in the paper were obtained by averaging over all the measurements.

The band-structure calculations were carried out by the spin-polarized relativistic (SPR) LMTO (linear muffin-tin orbital) method¹² within spin-density-functional theory with von Barth–Hedin parametrization¹³ of the exchange-correlation potential. To calculate the MOKE spectra of paramagnetic Pd, the term $2\mu_B \vec{B} \cdot \vec{s}$ which couples the spin of the electron to the external magnetic field was added to the Hamiltonian at the variational step, and a self-consistent solution was obtained. Then, the dispersion of the optical conductivity tensor $\sigma_{\alpha\beta}(\omega)$ was calculated from the energy-band structure by means of the Kubo-Greenwood¹⁴ linear-response expression¹⁵

$$\sigma_{\alpha\beta}(\omega) = \frac{-ie^2}{m^2 \hbar V_{uc}} \sum_{\mathbf{k}} \sum_{nn'} \frac{f(\epsilon_{n\mathbf{k}}) - f(\epsilon_{n'\mathbf{k}})}{\omega_{nn'}(\mathbf{k})} \times \frac{\Pi_{n'n}^\alpha(\mathbf{k}) \Pi_{nn'}^\beta(\mathbf{k})}{\omega - \omega_{nn'}(\mathbf{k}) + i\gamma}, \quad (1)$$

with V_{uc} the unit volume, $f(\epsilon_{n\mathbf{k}})$ the Fermi function, $\hbar\omega_{nn'}(\mathbf{k}) \equiv \epsilon_{n\mathbf{k}} - \epsilon_{n'\mathbf{k}}$ the energy difference of the Kohn-Sham energies $\epsilon_{n\mathbf{k}}$, and γ the inverse lifetime parameter, which is included to account for the finite lifetime of excited Bloch electron states. $\Pi_{nn'}^\alpha$ are the dipolar optical transition matrix elements, which in a fully relativistic description are given by

$$\Pi_{nn'}(\mathbf{k}) = m \langle \psi_{n\mathbf{k}} | c \boldsymbol{\alpha} | \psi_{n'\mathbf{k}} \rangle \quad (2)$$

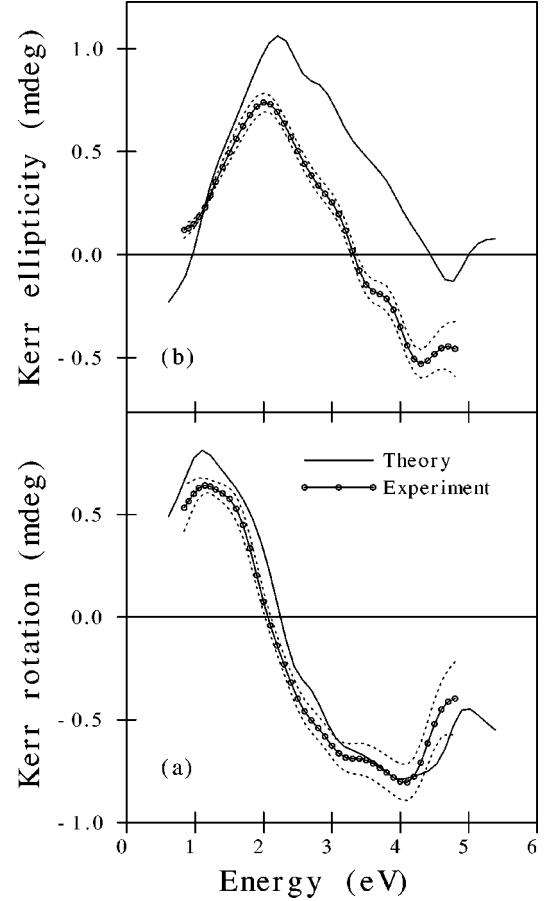


FIG. 1. Comparison between the experimental polar Kerr rotation (a) and ellipticity (b) spectra of a fcc Pd metal film measured in an applied field of 1.5 T, and the spectra calculated by the SPR LMTO method.

with $\psi_{n\mathbf{k}}$, the four-component Bloch electron wave function.

The averaged and smoothed experimental MOKE spectra of the Pd metal film (circles), with the variances indicated by dotted lines, are compared to the corresponding calculated spectra (solid line) in Fig. 1. The characteristic feature of the measured Pd Kerr rotation spectrum is a positive peak in the ir spectral range at ~ 1.2 eV and a negative two-peak structure in the uv range. The Kerr rotation and ellipticity in the ir and uv spectral range are of comparable magnitude, and do not overcome the value of $\sim 10^{-3}$ deg in the field of 1.5 T used. The Kerr rotation zero crossing at 2 eV corresponds to the peak in the ellipticity spectrum. As can be seen in Fig. 1, the agreement between the experimental and calculated polar Kerr rotation spectra is very good, both in the shape and the amplitude. The calculated Pd spectrum reproduces all the experimentally observed spectral features being slightly shifted to higher energies. For the Kerr ellipticity, a quantitative discrepancy between theory and experiment is somewhat larger; however, the shape of the spectra is reproduced well by the calculations. The value of the magnetic moment of $9.6 \times 10^{-4} \mu_B$ on the Pd atom obtained from the calculations agrees with the value of $\sim 1.0 \times 10^{-3} \mu_B$ per atom, as was estimated from the paramagnetic susceptibility data of Pd at 300 K.¹⁶

The calculated band structure of fcc Pd is shown in Fig. 2. In the absence of magnetic field, due to the time-reversal

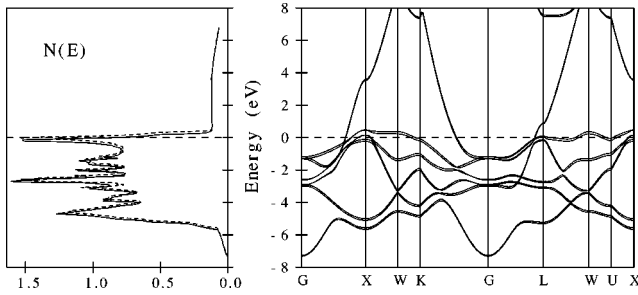


FIG. 2. Energy-band structure of fcc Pd in an external magnetic field of 240 T.

symmetry, all bands of Pd are at least twofold degenerated. The magnetic field lifts the degeneracy, but it is convenient to keep the numeration of the bands by pairs, adding a subscript if it is necessary to distinguish individual bands. Thus, in the following discussion, “transition $5 \rightarrow 6$ ” means the sum over the four possible transitions between the two pairs of bands, $5_{1,2}$ and $6_{1,2}$. In Fig. 2, the energy bands of fcc Pd, calculated for the induced moment of $0.2\mu_B$, are shown. We chose to plot the bands for strongly magnetized Pd, because the splitting of the bands due to the induced magnetization can be clearly visible in this case.

The appropriate discussion of electronic interband transitions underlying the MO effects studied requires an analysis of the spectral dependence of the optical conductivity tensor elements. It is well known that the MOKE spectra are determined by both the diagonal $\sigma_{\alpha\alpha}$ and off-diagonal $\sigma_{\alpha\beta}$ components of the conductivity tensor of a material. For a solid with at least threefold rotational symmetry, and in the polar geometry, the complex magneto-optical Kerr angle $\phi_K = \theta_K + i\eta_K$ is given by¹⁷

$$\phi_K = -\sigma_{xy}\sigma_{xx}^{-1}(1 + 4\pi i\omega^{-1}\sigma_{xx})^{-1/2}. \quad (3)$$

The absorptive parts of the optical conductivity tensor elements $\sigma_{xx}^{(1)}$ and $\sigma_{xy}^{(2)}$ are directly connected via Eq. (1) to the microscopic interband optical transitions.

As the absorptive parts of σ are additive quantities composed of interband transitions, to understand better the microscopic origin of the magneto-optical activity of Pd we performed the decomposition of the calculated absorptive part of the off-diagonal optical conductivity, $\sigma_{xy}^{(2)}$, into the contributions from separate interband transitions. The results of the analysis are presented in Fig. 3. As one can see from the figure, for photon energies up to 8 eV the $\omega\sigma_{xy}^{(2)}$ spectrum of Pd (solid line) is formed almost entirely by transitions between (3, 4, and 5) and (5 and 6) energy bands (full circles). Having a look at the band structure (Fig. 2), one can see that the initial states for these transitions, bands $3_{1,2}$, $4_{1,2}$, and $5_{1,2}$, are rather narrow bands predominantly of d character, while the final states $6_{1,2}$ are wide free-electron-like s - p bands. It should be pointed out that the dominant contribution, which determines the characteristic shape of the $\omega\sigma_{xy}^{(2)}$ spectrum with the negative peak at 1 eV and the two broad positive features within the range of 2–4 and at ~ 7 eV, comes from the $5 \rightarrow 6$ transitions. Moreover, it has been verified that the negative peak is formed by transitions from initial states within the energy range of ~ 0.5 eV below the Fermi level. Thus the zero crossing of the $\omega\sigma_{xy}^{(2)}$

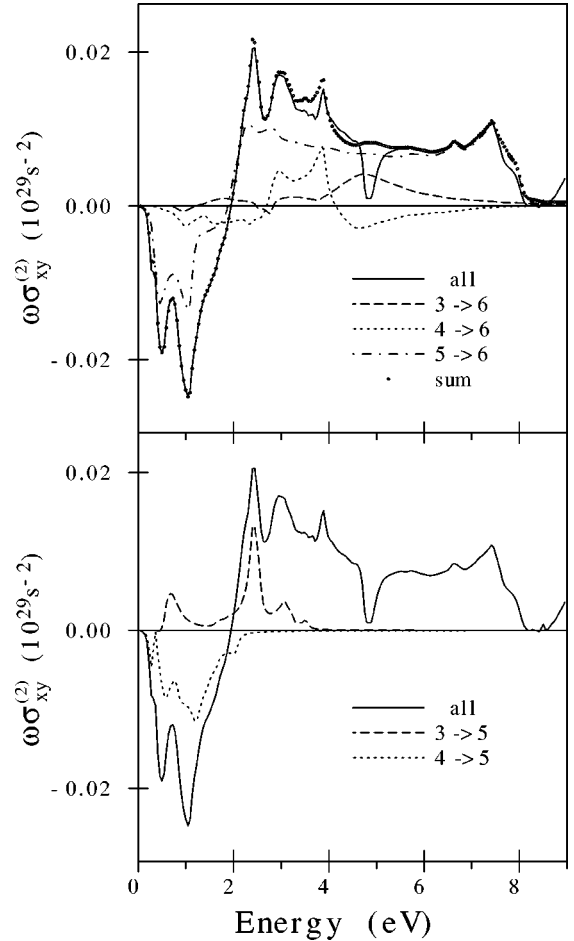


FIG. 3. Contributions of different interband transitions to the $\omega\sigma_{xy}^{(2)}$ spectrum of fcc Pd in an applied magnetic field of 1.5 T.

curve, observed at $\hbar\omega \approx 2$ eV, cannot be related to the maximum of the photoemission spectra observed at ~ -2 eV,¹⁸ as was supposed in Ref. 8.

It is illustrative to consider how the transitions between the individual bands (e.g., $5_1 \rightarrow 6_1$, and so on) sum up to form the curves shown in Fig. 3. As an example, in the following discussion the detailed analysis of the transitions between $5 \rightarrow 6$ energy bands will be performed. In Fig. 4, the contributions to the absorptive parts of the conductivity tensor, $\sigma_{xx}^{(1)}$ and $\sigma_{xy}^{(2)}$, from the four possible transitions ($5_1 \rightarrow 6_1$, $5_2 \rightarrow 6_2$, $5_1 \rightarrow 6_2$, and $5_2 \rightarrow 6_1$) between the fifth and sixth pairs of the bands are shown, together with their sums denoted as $5 \rightarrow 6$. Because the splitting of the bands is very small, the joint densities of states for the transitions are similar, and all the difference in the transitions’ intensities is due to the corresponding matrix elements.

Let us first consider the spin-flip transitions. As the spin-orbit coupling in Pd is relatively weak, the matrix elements of $5_1 \rightarrow 6_2$ and $5_2 \rightarrow 6_1$ transitions are significantly smaller than those of the remaining pair. In the limit of zero spin-orbit coupling strength, the band indexes 1 and 2 enumerate different projection of the electron spin, which is a good quantum number in this case, and the spin-flip $5_1 \rightarrow 6_2$ and $5_2 \rightarrow 6_1$ transitions are forbidden.

Considering the spin-up and down transitions, it is worth pointing out that the amplitudes of the $\omega\sigma_{xy,5_1-6_1}^{(2)}$ and

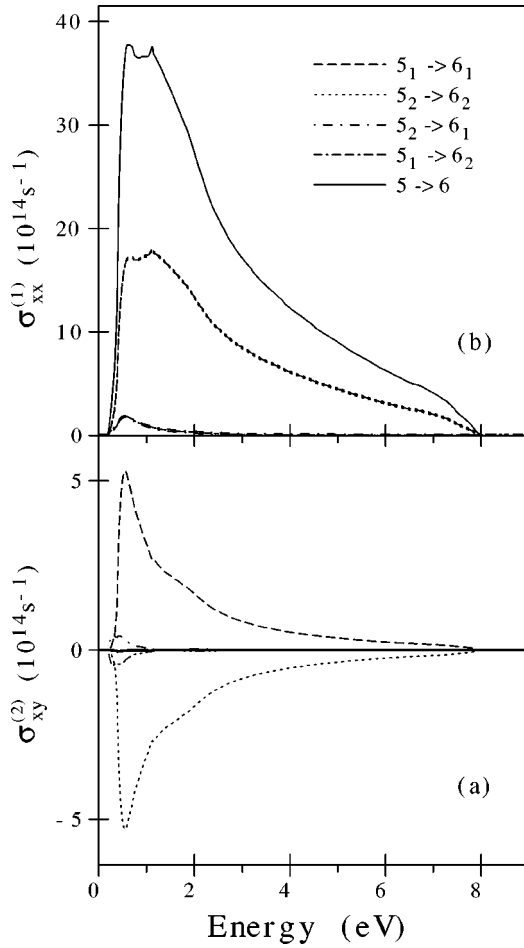


FIG. 4. Contributions of the individual transitions between the fifth and sixth pairs of bands to the $\sigma_{xy}^{(2)}$ (a) and $\sigma_{xx}^{(1)}$ (b) spectra of fcc Pd in an applied magnetic field of 1.5 T.

$\omega\sigma_{xy,5_2 \rightarrow 6_2}^{(2)}(\omega)$ spectra are only four times smaller than the amplitudes of the corresponding $\sigma_{xx}^{(1)}(\omega)$ spectra. However, as these spectra are of close shape and magnitude but of opposite sign, their sum $\sigma_{xy,5 \rightarrow 6}^{(2)}(\omega)$, plotted by the solid line in Fig. 4, is more than two orders of magnitude smaller at a magnetic field of 1.5 T. In other words, these transitions are responsible for the absorption of circularly left- and right- polarized light, respectively. In the absence of the magnetic field, bands $5_{1,2}$ and $6_{1,2}$ are degenerated, and the $\omega\sigma_{xy,5_1 \rightarrow 6_1}^{(2)}(\omega)$ and $\omega\sigma_{xy,5_2 \rightarrow 6_2}^{(2)}(\omega)$ spectra cancel exactly, leading to a zero MOKE. Due to the lifting of degeneracy caused by the magnetization, $\omega\sigma_{xy,5_1 \rightarrow 6_1}^{(2)}(\omega)$ and $-\omega\sigma_{xy,5_2 \rightarrow 6_2}^{(2)}(\omega)$ are no longer equal, and the resulting contribution of the transition $5 \rightarrow 6$ to $\sigma_{xy}^{(2)}(\omega)$ is given by a small-value difference of the two large quantities. It can be shown that, sufficiently far from the transition threshold, the difference is proportional to the shift in the energy positions of the constituent curves, i.e., to the average splitting ΔE of the fifth band. The splitting of the free-electron-like sixth band is much smaller, and can be neglected.

To model the MOKE spectra of strongly magnetized Pd, we performed the calculations increasing gradually the external field up to values as large as 480 T. Such a strong magnetic field cannot, of course, be obtained experimentally,

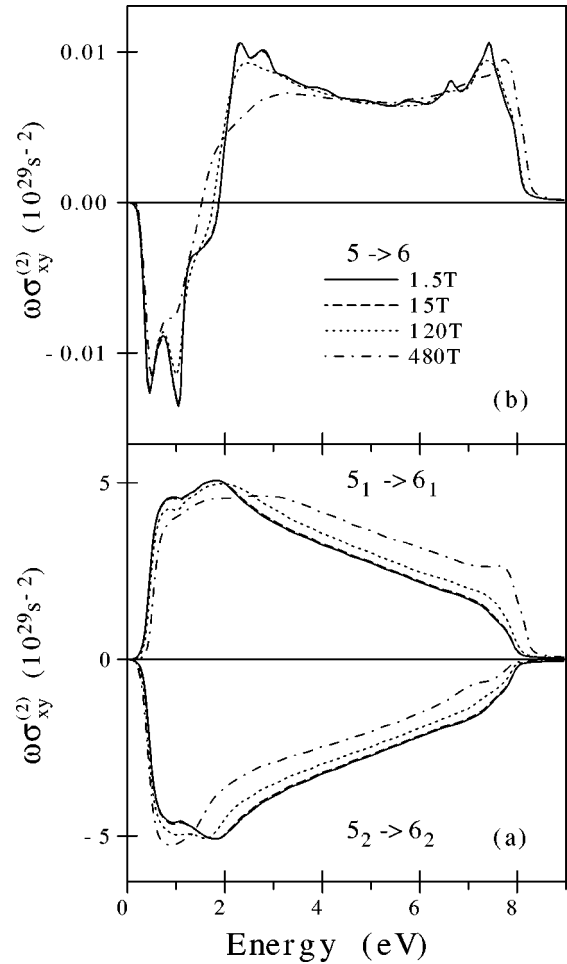


FIG. 5. The dependence of $\omega\sigma_{xy,5_1 \rightarrow 6_1}^{(2)}$ and $\omega\sigma_{xy,5_2 \rightarrow 6_2}^{(2)}$ components (a) and their sum, normalized vs the induced moment (see text) $\omega\sigma_{xy,5 \rightarrow 6}^{(2)}$ (b) on the value of the magnetic field applied to fcc Pd.

but it is necessary to induce a magnetic moment of $0.24\mu_B$ on the Pd atoms, which is close to the value observed in Pd-rich $\text{Fe}_x\text{Pd}_{1-x}$ and $\text{Co}_x\text{Pd}_{1-x}$ alloys. In agreement with the previous calculations,²⁰ a nonlinear dependence of the induced Pd moment on the applied magnetic field is observed for external fields larger than 100 T. However, the proportionality between the magnetization and amplitude of the MOKE spectra holds in the whole tested range of the external magnetic fields. To illustrate this, in Fig. 5 we plot the $\omega\sigma_{xy,5_1 \rightarrow 6_1}^{(2)}(\omega)$ and $\omega\sigma_{xy,5_2 \rightarrow 6_2}^{(2)}(\omega)$ components and their sum, $\sigma_{xy,5 \rightarrow 6}^{(2)}(\omega)$, for the selected values of the external field. The resulting $\sigma_{xy,5 \rightarrow 6}^{(2)}(\omega)$ spectra [Fig. 5(b)] have been normalized via a scaling down by a factor equal to the ratio of the calculated magnetic moment and the moment obtained at the field of 1.5 T. Whereas the differences between the $\omega\sigma_{xy,5_1 \rightarrow 6_1}^{(2)}(\omega)$ and $-\omega\sigma_{xy,5_2 \rightarrow 6_2}^{(2)}(\omega)$ components increase significantly with the magnitude of the magnetic field [Fig. 5(a)], the resulting normalized $\sigma_{xy,5 \rightarrow 6}^{(2)}(\omega)$ spectra are very close to each other above ~ 3 eV. The differences of the $\sigma_{xy,5 \rightarrow 6}^{(2)}(\omega)$ curves in the energy range between ~ 0.5 eV and ~ 3 eV are caused by transitions from those parts of the Brillouin zone in which the initial states are located within the value of ΔE near the Fermi energy, e.g., around the L

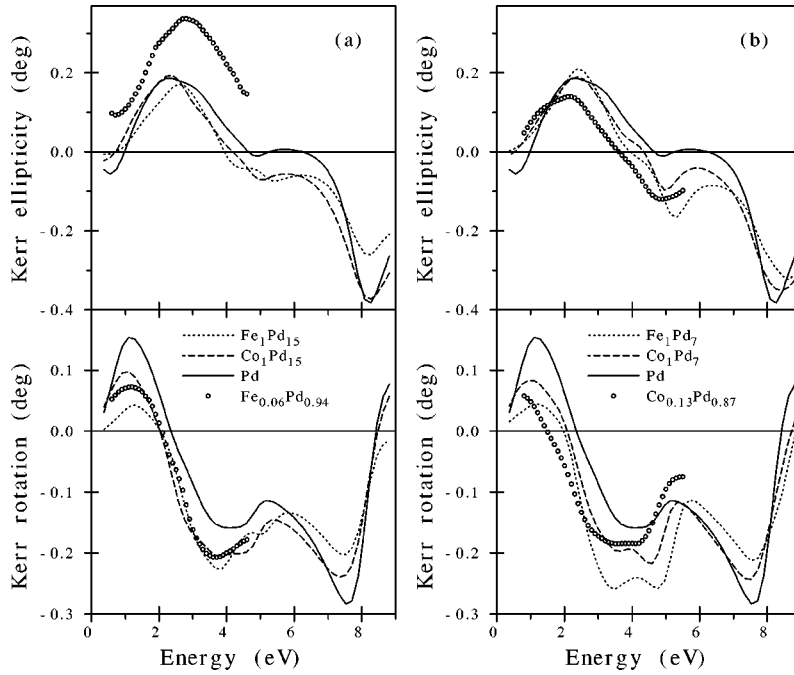


FIG. 6. Experimental (open circles) and theoretical (dashed and dotted lines) MOKE spectra of Pd-rich alloys with 3d transition metals. The calculated MOKE spectra of fcc Pd in an external field of 480 T, which induces a magnetic moment of $0.24\mu_B$, are plotted by solid lines.

symmetry point (see Fig. 2). As only one of the two splitted bands is occupied in this case, the contribution of these transitions to $\sigma_{xy}^{(2)}$ is proportional to $\sigma_{xy,5_1 \rightarrow 6_1}^{(2)}$ itself, instead of to the sum of $\omega\sigma_{xy,5_1 \rightarrow 6_1}^{(2)}$ and $\omega\sigma_{xy,5_2 \rightarrow 6_2}^{(2)}$. A similar scaling of $\sigma_{xy}^{(2)}$ with the magnetic moment was also found for the other interband transitions. The reason for the scaling is that, as already mentioned, the magnitude of the $\sigma_{xy}^{(2)}$ spectra is proportional to the splitting ΔE of the bands degenerated in the absence of the external field. The splitting, in turn, is proportional to the induced magnetic moment, as long as ΔE is much smaller than the width of the d band, which is fulfilled in the case of Pd.

III. MAGNETO-OPTICAL PROPERTIES OF PALLADIUM IN DILUTED ALLOYS

In Ref. 8, the MOKE spectra of $\text{Fe}_{0.06}\text{Pd}_{0.94}$ alloy were considered for a discussion of the MO properties of the spin-polarized Pd. It is interesting to investigate to what extent the MOKE spectra of Pd-rich alloys with 3d transition metals are governed by the MO activity of Pd. For this study, we used the available MOKE spectra of Pd-rich Fe-Pd and Co-Pd alloys. The $\text{Fe}_{0.06}\text{Pd}_{0.94}$ spectra,⁸ and our results for the $\text{Co}_{0.13}\text{Pd}_{0.87}$ alloy film,¹⁹ are shown in Fig. 6. As can be seen, the overall shape of the $\text{Fe}_{0.06}\text{Pd}_{0.94}$ Kerr rotation spectrum is similar to that of the $\text{Co}_{0.13}\text{Pd}_{0.87}$ spectrum; nevertheless the fine features are different. The uv peak in the spectrum of the $\text{Fe}_{0.06}\text{Pd}_{0.94}$ alloy is sharper, and shifted in the energy position as compared to the spectrum of $\text{Co}_{0.13}\text{Pd}_{0.87}$ alloy. Also, a slightly larger positive rotation is observed for $\text{Fe}_{0.06}\text{Pd}_{0.94}$ in the ir range. Comparing the spectra of the alloys to the MOKE spectra of paramagnetic Pd (see Fig. 1), one can note that the overall shape of the spectra is strikingly similar. The largest difference is observed for the ratio of ir and uv peak amplitudes; the ratio for Pd is about two times larger than that for the alloys. Notwithstanding the fact that the amplitude of the Pd spectra is about 200 times smaller

than that of the alloys, the positions of the uv peak differ only slightly. This leads one to the conclusion that the MOKE spectra of the Pd-rich alloys with magnetic 3d metals are mainly determined by the MO properties of the spin-polarized Pd. However, the contribution from the 3d atoms is substantial, especially in the ir spectral range, in which the polar Kerr rotation in both Fe and Co metals is negative.

The conclusion that 3d transition atoms make only relatively small contributions to the MO spectra of Pd-rich alloys is, also, supported by the results of *ab initio* calculations. The MOKE spectra calculated for the model alloys $\text{Co}_1\text{Pd}_{15}$, $\text{Fe}_1\text{Pd}_{15}$, Co_1Pd_7 , and Fe_1Pd_7 , and for fcc Pd in the external field of 480 T, are compared to the experimental ones in Fig. 6. For all the alloys, the cubic supercells have been constructed with a lattice constant equal to that of fcc Pd. The magnetic moment of $0.24\mu_B$, induced on the Pd atom by a field of 480 T, is close to the average Pd moment calculated for $\text{Fe}_1\text{Pd}_{15}$ ($0.22\mu_B/\text{atom}$) and $\text{Co}_1\text{Pd}_{15}$ ($0.25\mu_B/\text{atom}$) alloys. As can be seen from Fig. 6, the theoretical MOKE spectra are in good agreement with the experimental spectra of the alloys of correspondingly close composition. The only exception is the Kerr ellipticity spectrum of the $\text{Fe}_{0.06}\text{Pd}_{0.94}$ alloy, which, being of similar shape, is shifted upward with respect to the calculated one. The calculated MOKE spectra of $\text{Fe}_1\text{Pd}_{15}$ and $\text{Co}_1\text{Pd}_{15}$ alloys and strongly magnetized Pd metal are very close to each other [see Figs. 6(a) and 6(b)], and, as could be supposed in advance, differences between the spectra become more pronounced with an increase of the 3d metal content. However, strictly speaking, the subtle modification of the calculated MOKE spectra due to the presence of 3d atoms are still observed even for the diluted $\text{Fe}_1\text{Pd}_{15}$ and $\text{Co}_1\text{Pd}_{15}$ alloys. It can be concluded that the MO spectra of Pd-based alloys in the limit of a small concentration of magnetic 3d atoms can be considered only as a first approximation of the magneto-optical response of spin-polarized palladium. When the amount of the magnetic 3d atoms increases, the contribution to the alloys' spectra, coming from the 3d atoms and the

effects of the hybridization of the Pd $4d$ with the $3d$ states of transition metals, results in appreciable differences between the Pd and alloys' spectra. The role of the $3d$ - $5d$ hybridization in the formation of the MO spectra of Co-Pt compounds was studied in our previous paper.¹¹ The same considerations concerning the importance of the $3d$ - $4d$ hybridization effects are applicable to the case of the MO spectra of Pd-rich alloys, keeping in mind that the spin-orbit coupling in Pd is three times weaker than in Pt.

IV. CONCLUSIONS

The magneto-optical response of the paramagnetic fcc Pd metal film measured in an external magnetic field of 1.5 T over a photon energy range $0.8 < \hbar\omega < 4.8$ eV was presented. Band-structure and MOKE spectra calculations of paramagnetic Pd have been performed by the spin-polarized relativistic LMTO method within the spin-density-functional theory, with the term $2\mu_B \vec{B} \cdot \vec{s}$ added to the Hamiltonian which couples the spin of the electron to the external magnetic field. The calculations reproduced the experimentally observed Pd MOKE spectra in a very satisfactory way, and explained their microscopic origin. A band-by-band decomposition of the fcc Pd MO spectra has been performed, and the transitions responsible for the prominent structures in the spectra have been identified. The dominant role of transitions

from states in the vicinity of the Fermi level in the formation of Pd MOKE spectra was found. It has been found and explained in terms of the band splitting that the proportionality between the magnetization and magnitude of the Pd MOKE spectra holds in the whole tested range of external magnetic fields up to 480 T.

Finally, from a comparison of the MOKE spectra of a Pd metal film measured in an applied field of 1.5 T with the spectra of Pd-rich alloys with magnetic $3d$ metals, and from the results of first-principles calculations, a conclusion was derived that the MO properties of magnetized Pd depend only weakly on the source of the magnetization. Whether the magnetic moment on the Pd atom is induced by the external field or by the hybridization with the magnetic $3d$ atoms, the Pd contribution to the MOKE spectra remains almost the same.

ACKNOWLEDGMENTS

This work was supported by the Polish State Committee for Scientific Research (KBN) under Contract No. 2 P03B 113 11. V.N.A., A.N.Y., and A.Ya.P. would also like to acknowledge support by the German Federal Ministry for Education, Science, Research and Technology within the program TRANSFORM (Förderkennzeichen: 03N9006).

*Permanent address: Institute of Metal Physics, 36 Vernadskii Street, 252142 Kiev, Ukraine.

†Author to whom correspondence should be addressed. Electronic address: ubaluba@alpha.fuw.edu.pl

¹K. Sato, H. Ikekame, Y. Tosaka, and S.-C. Shin, *J. Magn. Magn. Mater.* **126**, 553 (1993); S. Uba, L. Uba, and R. Gontarz, *IEEE Trans. Magn.* **MAG-30**, 806 (1994); H. Brändle, D. Weller, J. C. Scott, S. S. P. Parkin, and C.-J. Lin, *ibid.* **MAG-28**, 2967 (1992); K. Sato, H. Hongu, H. Ikekame, J. Watanabe, K. Tsuzuki, Y. Togami, M. Fujisawa, and T. Fukazawa, *Jpn. J. Appl. Phys., Part. 1* **31**, 3603 (1992).

²C.-J. Lin, G. L. Gorman, C. H. Lee, R. F. C. Farrow, E. E. Marinero, H. V. Do, H. Notarys, and C. J. Chien, *J. Magn. Magn. Mater.* **93**, 194 (1991); K. Spörl and D. Weller, *ibid.* **93**, 379 (1991).

³D. Weller, W. Reim, K. Spörl, and H. Brändle, *J. Magn. Magn. Mater.* **93**, 183 (1991); K. Sato, H. Ikekame, Y. Tosaka, K. Tsuzuki, Y. Togami, and M. Fujisawa, *ibid.* **126**, 572 (1993).

⁴E. E. Fullerton, D. Stoeffler, K. Ounadjela, B. Heinrich, Z. Celinski, and J. A. C. Bland, *Phys. Rev. B* **51**, 6364 (1995); J. Vogel, A. Fontaine, V. Cros, F. Petroff, J.-P. Kappler, G. Krill, A. Rogalev, and J. Goulon, *ibid.* **55**, 3663 (1997); O. Rader, E. Vescovo, J. Redinger, S. Blügel, C. Carbone, W. Eberhardt, and W. Gudat, *Phys. Rev. Lett.* **72**, 2247 (1994).

⁵R. M. Bozorth, P. A. Wolff, D. D. Davis, V. B. Compton, and J. H. Wernick, *Phys. Rev.* **122**, 1157 (1961); J. W. Cable, E. O. Wollan, and W. C. Koehler, *ibid.* **138**, A755 (1965).

⁶V. L. Moruzzi and P. M. Marcus, *Phys. Rev. B* **39**, 471 (1989); H. Chen, N. E. Brener, and J. Callaway, *ibid.* **40**, 1443 (1989).

⁷R. Lässer and N. V. Smith, *Phys. Rev. B* **25**, 806 (1982); N. E. Christensen, *ibid.* **14**, 3446 (1976); A. Oswald, R. Zeller, and P. H. Dederichs, *Phys. Rev. Lett.* **56**, 1419 (1986).

⁸W. Reim, H. Brändle, D. Weller, and J. Schoenes, *J. Magn. Magn. Mater.* **93**, 220 (1991).

⁹P. M. Oppeneer, T. Maurer, J. Sticht, and J. Kübler, *Phys. Rev. B* **45**, 10 924 (1992); S. Uba, L. Uba, R. Gontarz, V. N. Antonov, A. Ya. Perlov, and A. N. Yaresko, *J. Magn. Magn. Mater.* **140-144**, 575 (1995); G. Y. Guo and H. Ebert, *Phys. Rev. B* **51**, 12 633 (1995); S. Uba, L. Uba, A. Ya. Perlov, A. N. Yaresko, V. N. Antonov, and R. Gontarz, *J. Phys.: Condens. Matter* **9**, 447 (1997); P. M. Oppeneer and V. N. Antonov, in *Spin-Orbit Influenced Spectroscopies of Magnetic Solids*, edited by H. Ebert and G. Schütz (Springer, Heidelberg, 1996) pp. 29–47; S. Uba, L. Uba, A. N. Yaresko, A. Ya. Perlov, V. N. Antonov, and R. Gontarz, *J. Phys.: Condens. Matter* **10**, 3769 (1998).

¹⁰R. Gontarz and T. Lucinski, *J. Magn. Magn. Mater.* **101**, 253 (1991).

¹¹S. Uba, L. Uba, A. N. Yaresko, A. Ya. Perlov, V. N. Antonov, and R. Gontarz, *Phys. Rev. B* **53**, 6526 (1996).

¹²V. N. Antonov, A. Ya. Perlov, A. P. Shpak, and A. N. Yaresko, *J. Magn. Magn. Mater.* **146**, 205 (1995).

¹³U. von Barth and L. Hedin, *J. Phys. C* **5**, 1629 (1972).

¹⁴R. Kubo, *J. Phys. Soc. Jpn.* **12**, 570 (1957).

¹⁵C. S. Wang and J. Callaway, *Phys. Rev. B* **9**, 4897 (1974).

¹⁶F. E. Hoare and J. C. Matthews, *Proc. R. Soc. London, Ser. A* **212**, 137 (1952).

¹⁷W. Reim and J. Schoenes, in *Ferromagnetic Materials*, edited by K. H. J. Buschow and E. P. Wohlfarth (North-Holland, Amsterdam, 1990), Vol. 5, p. 133.

¹⁸J.-S. Kang, D. W. Hwang, C. G. Olson, S. J. Youn, K.-C. Kang, and B. I. Min, *Phys. Rev. B* **56**, 10 605 (1997).

¹⁹S. Uba, A. N. Yaresko, L. Uba, A. Ya. Perlov, V. N. Antonov, and R. Gontarz, *Phys. Rev. B* **57**, 1534 (1998).

²⁰A. Hjelm, in *Proceedings of the International Conference on the Physics of Transition Metals 1992*, edited by P. M. Oppeneer and J. Kübler (World Scientific, Singapore, 1993), pp. 275–278.